Journal of
Plankton Research

academic.oup.com/plankt

J. Plankton Res. (2023) 45(4): 604–613. First published online June 9, 2023 https://doi.org/10.1093/plankt/fbad019

ORIGINAL ARTICLE

Thermal niche of the dinoflagellate *Karlodinium veneficum* across different salinity and light levels

NAYANI K. VIDYARATHNA*, SO HYUN (SOPHIA) AHN AND PATRICIA M. GLIBERT

UNIVERSITY OF MARYLAND CENTER FOR ENVIRONMENTAL SCIENCE, HORN POINT LABORATORY, 2020 HORNS POINT RD, CAMBRIDGE, MD, USA

*CORRESPONDING AUTHOR: nvidyarthna@umces.edu

Received December 5, 2022; editorial decision April 5, 2023; accepted April 5, 2023

Corresponding editor: Lisa Campbell

The interactive effects of temperature (15–30°C), salinity (5–30) and light (low-100 and high-300 μmol photons m^{-2} s^{-1}) on growth, thermal niche properties and cellular carbon (C) and nitrogen (N) of the toxic dinoflagellate, *Karlodinium veneficum*, were studied to understand its potential for change under future climate conditions in the eutrophic Chesapeake Bay. Cell growth was highest under conditions of 25–28°C, salinity 10–20 and high light, which represented the preferred physical niche for bloom formation in the present day. In the Chesapeake Bay, blooms generally occur at 25–29°C and salinity 10–14, while low-biomass occurrences have been found at salinities 15–29, consistent with the laboratory findings. High light increased the thermal sensitivity of *K. veneficum* and lowered the thermal optima for growth. Under conditions of low light, and salinity 10–20, cells exhibited the highest thermal optima for growth. The highest upper thermal maxima were observed at salinity 30, suggesting that cells in the lower estuary would be more thermally resistant than those in upper and mid-estuarine regions, and therefore these higher salinity regions may provide over-summering habitats for *K. veneficum*. Cellular C and N were highly varied at the preferred salinity and temperature niche and C:N ratios showed decreasing trends with temperature.

KEYWORDS: harmful algal blooms; *Karlodinium veneficum*; climate change; thermal niche properties; cellular C and N

Downloaded from https://academic.oup.com/plankt/article/45/4/604/7192951 by National Oceanic & Atmospheric Administration user on 18 March 2025

available online at academic.oup.com/plankt

© The Author(s) 2023. Published by Oxford University Press. All rights reserved. For permissions, please e-mail: journals.permission@oup.com

INTRODUCTION

The Chesapeake Bay, the largest estuary in the USA, is predicted to experience significant non-linear changes in climate forcing. These changes include increases in water temperature and changes in salinity and carbonate chemistry by the end of the 21st century (Najjar *et al.*, 2010; Hong and Shen, 2012; Muhling *et al.*, 2018; Shen *et al.*, 2020; Li *et al.*, 2020a). Mean temperatures may rise by as much as 2–5.5°C. Salinity changes are more complex. While increased precipitation may reduce the salinity in the upper bay regions, sea level rise will increase saltwater intrusion and salinity in the lower bay regions (Hong and Shen, 2012; Ni *et al.*, 2020) producing strong salinity gradients across the bay and a salinity squeeze for those organisms with a narrow salinity tolerance. Due to altered precipitation patterns, springs in the Bay are expected to become wetter which will lead to increases in nutrient loads (Howarth, 2008; Wagena *et al.*, 2018). Changes in the streamflow and associated suspended solid loadings may also change the light penetration directly affecting the phytoplankton growth and physiology, in turn causing feedback effects on light penetration in the water column (Testa *et al.*, 2019). Carbonate chemistry in the Bay is also spatially and temporally complex. The upper Bay is showing trends of alkalinification due to changing freshwater input and increased alkalinity from rivers, while the lower Bay is experiencing acidification due to ocean acidification (Kaushal *et al.*, 2013; Li *et al.*, 2020a). Among major outcomes of the potential climate-change impacts in the Chesapeake Bay is an increase of harmful algal bloom (HAB) occurrence and changes in their seasonal and spatial distribution (Najjar *et al.*, 2010; Li *et al.*, 2020b; Glibert *et al.*, 2022).

The harmful dinoflagellate, *Karlodinium veneficum*, is among the common HAB species that have historically been present and are increasing in abundance and extent in the Chesapeake Bay (Li *et al.*, 2000a, 2015; Marshall *et al.*, 2005; Lin *et al.*, 2018a). Blooms of *K. veneficum* have also been documented worldwide from Namibia (Braarud, 1957) to Europe (Bjørnland and Tangen, 1979), China (Dai *et al.*, 2014) and Australia (Adolf *et al.*, 2015). This species produces a suite of toxic compounds called karlotoxins (KmTx) with cytotoxic, ichthyotoxic, hemolytic and grazer deterrent properties (Deeds *et al.*, 2002; Adolf *et al.*, 2007; Waggett *et al.*, 2008; Fu *et al.*, 2010; Place *et al.*, 2012). Blooms often cause massive fish kills and may be toxic to oyster embryos, larvae and juveniles (Adolf *et al.*, 2007; Glibert *et al.*, 2007; Brownlee *et al.*, 2008; Stoecker *et al.*, 2008; Waggett *et al.*, 2008). Detailed spatial surveys and long-term monitoring data from the Bay show that *K. veneficum* occurrence is more prevalent across mid and upper regions of the Chesapeake Bay, where salinity is in the range of 7–17 and during late summer when the temperature is typically over 25°C (Li *et al.*, 2000a, 2015; Lin *et al.*, 2018a).

Based on the long-term trends and the inter-annual variabilities of *K. veneficum* occurrence, and physio-chemical parameters and hydrology of the Chesapeake Bay, a recent habitat suitability model (Li *et al.*, 2020b) provided important insights with respect to temporal and spatial distribution of *K. veneficum* blooms in a future climate. According to this model, temporal changes in a future climate for *K. veneficum* are largely a function of temperature, while spatial changes are a function of salinity (Li *et al.*, 2020b). This habitat model further predicts that higher summer temperatures due to warming may exceed the preferred growth temperature of *K. veneficum*, the result of which may be to reduce bloom occurrence in the summer and prolong the potential bloom season in the spring and autumn (Li *et al.*, 2020b). Furthermore, *K. veneficum* shifts downstream during wetter years and upstream during the dry years. In this model, the physical niche was constrained to a range of temperature of 21–30°C and salinity of 5–12, based on literature from the Bay and elsewhere (reviewed in Li *et al.*, 2020b). However, *K. veneficum* can grow over a broader range of temperatures, 7–30°C, and salinities, 5–30 than defined by the habitat model (Nielsen, 1996; Adolf *et al.*, 2009; Place *et al.*, 2012; Li *et al.*, 2015; Vidyarathna *et al.*, 2020).

Most laboratory studies that have reported growth responses of *K. veneficum* across a range of temperatures (e.g. Lin *et al.*, 2018b; Vidyarathna *et al.*, 2020) have been conducted at a single salinity and light condition. However, temperature responses are altered by the resource availability (e.g. light and nutrients). For example, under light limitation, phytoplankton growth, including *K. veneficum*, may be less sensitive to temperature than under light-saturated conditions (Raven and Geider, 1988; Edwards *et al.*, 2016; Coyne *et al.*, 2021). The thermal response of an individual species is characterized as a thermal niche, with its lower and upper thermal boundaries and optimum temperature at which growth (or other trait values) is maximized.

This study investigated the response of thermal niche of *K. veneficum* and its cellular C and N quotas across a range of salinities under low (LL) and high light (HL) conditions. Thermal reaction norms were used to quantify the responses of *K. veneficum* growth to temperature and to extract parameters of their thermal niche at each combination of salinity and light in order to test the hypothesis that growth at the preferred salinity niche (i.e. 5–12, Li *et al.*, 2020b) will display higher thermal optima than growth outside of the preferred niche, and

Downloaded from https://academic.oup.com/plankt/article/45/4/604/7192951 by National Oceanic & Atmospheric Administration user on 18 March 2025

that under light-limited conditions, growth will have lower thermal optima than growth at light-saturated conditions. Results were compared to recent *in situ* data from the Chesapeake Bay.

MATERIALS AND METHODS

Algal cultures and experimental design

Karlodinium veneficum (CCMP 1975; National Center for Marine Algae and Microbiota, Bigelow, USA), originally isolated from the Chesapeake Bay, Maryland, USA, was first grown in non-axenic batch cultures in f/2 media (882 μM NO_3^- and 36 μM PO_4^{3-}, Guillard and Ryther, 1962) at 20°C under a light intensity of 100 μmol photons m^{-2} s^{-1} (provided by LED bulbs) on a 12:12-hour light:dark cycle. The seawater used for media preparation was collected from Wachapreague, VA, and diluted to the respective salinity levels with laboratory-grade fresh water (18 MΩ) followed by filtration (Whatman 0.7 μm nominal pore size) and autoclaved.

The growth experiments were conducted across a gradient of temperature and salinity at two light intensities using a 5 × 5 × 2 factorial design. Five temperature levels (15, 20, 25, 28 and 30°C) and five salinity levels (5, 10, 15, 20 and 30) were chosen to span the temporal and spatial range at which most *K. veneficum* blooms occur in the Chesapeake Bay (Li *et al.*, 2015; Lin *et al.*, 2018a). Light intensities were 100 μmol photons m^{-2} s^{-1} (LL) and 300 μmol photons m^{-2} s^{-1} (HL). All treatments were conducted in quadruplicate 50 mL tubes with initial culture volumes of 40 mL. Experiments were started with exponentially growing cultures under optically thin conditions with cell densities ranging from 2000 to 5000 cells mL^{-1}.

The cultures that were originally grown in the salinity 15 media were slowly (over three generations) transferred to the next higher or lower salinity. The newly acclimated cultures were subsequently transferred to the next salinity following the same procedure. Once they reached the target salinity level, they were slowly adjusted to target temperature(s), by initially shifting them from 20°C to either 15 or 25°C by changing the temperature at a rate of 0.5°C day^{-1} in walk-in temperature-controlled incubators. Cultures were then re-inoculated into the fresh media and were further acclimated for at least four generations before measurements after 4–7 days of subsequent growth at the exponential phase.

Before conducting the experiments at the HL condition, salinity- and temperature-acclimated cultures were shifted to higher light at a daily rate of 50 μmol photons m^{-2} s^{-1} until 300 μmol photons m^{-2} s^{-1}, followed by at least two generations of acclimation at HL.

Algal growth was followed by measuring *in vivo* chlorophyll *a* (chl *a*) fluorescence (TD 700; Turner Designs, USA) of the whole cultures daily until they reach the late exponential phase (4–7 days). Specific growth rates (μ, day^{-1}) were calculated based on the fluorescence during the exponential growth phase using the following formula:

$$\mu = \frac{(\ln N_2 - \ln N_1)}{(t_2 - t_1)} \quad (1)$$

where N_1 and N_2 are *in vivo* chl *a* fluorescence at time t_1 and t_2. Experiments were terminated when cultures reached late exponential phase growth, and the samples were collected for analyses of final cell density, and cellular carbon (C) and nitrogen (N).

Subsamples (1 mL) of each replicate were preserved with acid Lugol's solution (final concentration 2% v/v) and were counted using a 0.1-mm Neubauer hemocytometer using a light microscope at ×100 magnification.

Cellular carbon and nitrogen

Samples (15 mL) for cellular organic C and N were filtered onto 25 mm pre-combusted glass-fiber filters (2 h at 450°C, GF/F, Whatman), dried at 60°C for 24 h and then stored in a desiccator prior to analyses. Cellular C and N were then quantified with a CHN elemental analyzer (ECS 4010 Elemental combustion system; Costech Instruments, USA), with phenylalanine and EDTA used as standards.

Chesapeake Bay monitoring data

The relationship of *in situ* bloom occurrence with temperature and salinity across the Chesapeake Bay for the period of 2016–2017 was analyzed using *K. veneficum* cell density and water quality data obtained from the Chesapeake Bay program (https://www.chesapeakebay.net/what/data). Temperature and salinity for each bloom record were extracted from the water quality data. The severity of blooms was defined based on algal biomass according to Li *et al.* (2015). Briefly, blooms were grouped into three types: Type I (>5 × 10^5 cells L^{-1}), Type II (5 × 10^5–1 × 10^5 cells L^{-1}) and Type III (1 × 10^5–1 × 10^3 cells L^{-1}). The records of each bloom type were binned into six different temperature ranges (<10, 10–14, 15–19, 20–24, 25–29 and >30°C respectively) and salinity ranges (<5, 5–9, 10–14, 15–19, 20–29 and > 30 respectively) and the percent frequency of bloom (Types I, II and III) occurrence at each temperature and salinity range was calculated.

Downloaded from https://academic.oup.com/plankt/article/45/4/604/7192951 by National Oceanic & Atmospheric Administration user on 18 March 2025

Data analyses

Statistical analyses were performed using R statistical software (v 32021.09.0; R Core Team, 2021). The data were checked for normality with the Shapiro–Wilk test, while homogeneity of the variances was assessed with the Bartlett test.

Karlodinium veneficum growth vs temperature curves at each salinity and light combinations were analyzed using the double-exponential model (Thomas *et al.*, 2017),

$$\mu(T) = b_{1.} \cdot \exp(b_2 . T) - (d_0 + d_1 \cdot \exp(d_2 \cdot T) \quad (2)$$

where $\mu(T)$is the growth rate (day^{-1}), $b_{1.}$ is the birth rate at 0°C, b_2 is the exponential increase in birth rate (i.e. gross growth rate) with increasing temperature, d_0 is the temperature-independent mortality term and d_1 and d_2 jointly describe the exponential increase in mortality rate with temperature. Thus, the first half of equation (2) describes the effect of temperature on birth rates, while the second half describes the mortality rates.

The data were fit to equation (2) using non-linear least square regression using the *R* packages, "*rTPC*" and "*nls.multstart*" (Padfield *et al.*, 2021). Model confidence intervals were calculated by non-parametric bootstrapping, "case" (999 replicates) by using the "Boot" function in the "*car*" package in R (Fox and Weisberg, 2011). The key parameters of the model fits were extracted using the helper function in "*rTPC*" package. The parameters *Topt*, the optimum temperature for growth, and *CTmax*, the upper thermal niche limit for the growth of *K. veneficum* under each salinity-light combination, were extracted for further downstream analyses. 95% confidence intervals for *Topt* and *CTmax* were also calculated by the non-parametric bootstrapping, "case" (200 replicates) as described above.

Maximum growth rates and molar C:N ratios of *K. veneficum* across the temperature and salinity gradients at LL and HL were statistically compared using one-way and two-way analysis of variance (ANOVA) followed by Tukey HSD post hoc tests in R.

RESULTS

Growth rates and thermal niche properties

Growth of *K. veneficum* as a function of temperature displayed a left-skewed unimodal growth pattern under all salinity and light conditions (Fig. 1, Table SI). Highest growth rates were found for cells grown at the mid-salinity (10–20) range and at 20–28°C (Fig. 1, Table SI). Growth was significantly higher under HL than under LL for the cells grown at 20°C (Tukey's HSD, $P = 0.002$, 0.04 and 0.01 for salinity 5, 10 and 15 respectively), at 25°C (Tukey's HSD, $P = 0.007$ and <0.001 for salinity 5 and 30 respectively) and at 28°C (Tukey's HSD, $P = 0.002$ and 0.006 for salinity 10 and 30). Growth rates ranged from 0.11 to 0.44 day^{-1} under LL, and from 0.10 to 0.68 day^{-1} under HL. The cells did not grow at salinity 5 and temperature 30°C at LL, and at both salinity 5 and 10 at 30°C at HL. When growth rates under each light level were evaluated separately, significant interaction effects between temperature and salinity were found for both LL and HL (two-way ANOVA, $P < 0.001$).

Calculated *Topt* for *K. veneficum* across the salinities from 5–30 ranged from 25.0 to 27.5°C under LL, while it ranged from 23.7 to 26.6°C under HL (Fig. 2, Table SII). The highest *Topts* were found at salinity 10 and 15 (27.5°C) under LL and at salinity 10 (26.6°C) under HL. Although growth rates were generally higher at HL at salinities below 30, the *Topt* for each salinity was generally higher at LL than at HL. The upper thermal niche limit (*CTmax*), on the other hand, showed little variance across the salinity range of 5–30 and ranged from 30.0 to 31.8°C under LL and from 30.0 to 31.6°C under HL. At the highest salinity level (salinity 30), the cells were more resilient to temperature increases when they were at the LL condition as indicated by the relatively higher *CTmax* for salinity 30 under LL (Fig. 2, Table SII). At the mid-salinity range (15–20), cells were more resilient to temperature increases under HL conditions as indicated by slightly higher *CTmax* found for HL grown cells compared to those grown at LL.

Cellular carbon and nitrogen

Growth temperature, salinity and light also affected the stoichiometry of cellular C and N (Fig. 3, Table SIII). Molar C:N ratios were invariant across the temperature range, 15–30°C and both light levels at the two extreme salinity levels (5 and 30), being well below the Redfield ratio of 6.6 (Fig. 3). At salinity 10, cells grown at LL and below 30°C had significantly higher C:N ratios than those at HL (two-way ANOVA, $P = 0.003$), while temperature had minimal effect. However, at salinity 15, both temperature and light had significant effects on C:N ratios (two-way ANOVA, $P < 0.001$ for both temperature and light). Also, a significant interaction effect between temperature and light on C:N ratios were found at salinity 15 (two-way ANOVA, $P < 0.001$). Under LL, the highest C:N ratios were found for 15 and 20°C (Tukey's HSD, $P < 0.05$ compared to 25 and 30°C), while under HL, C:N ratios were invariant across temperature. Furthermore, except at 25 and 30°C, C:N ratios at LL were significantly higher than those at HL (Tukey's HSD, $P = 0.001$, <0.001 and 0.008 for 15, 20 and 28°C respectively). At salinity 20,

Downloaded from https://academic.oup.com/plankt/article/45/4/604/7192951 by National Oceanic & Atmospheric Administration user on 18 March 2025

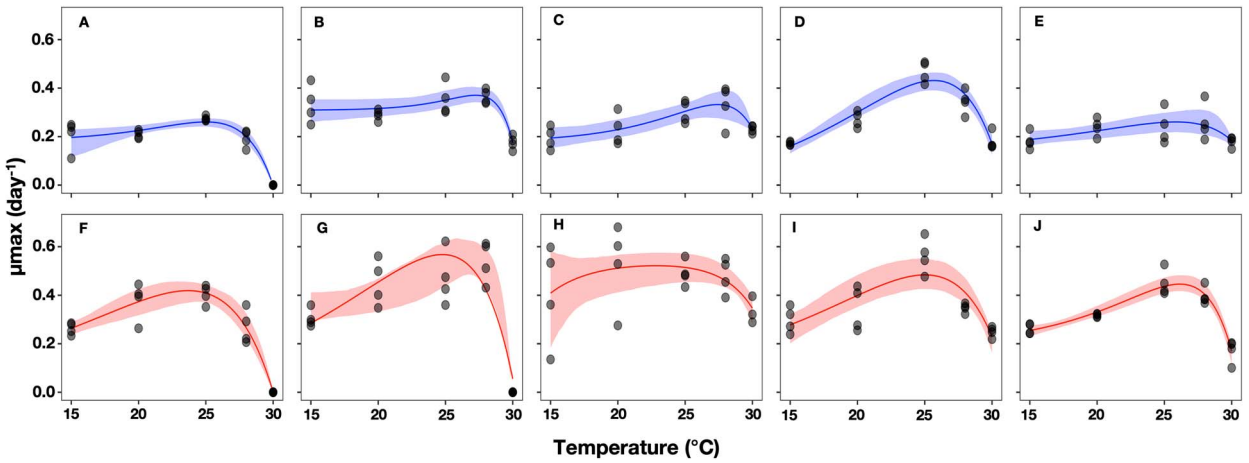

Fig. 1. Maximum growth rates (μmax, day^{-1}) of *K. veneficum* across the temperature range of 15–30°C at salinity 5 (**A**, **F**), 10 (**B**, **G**), 15 (**C**, **H**), 20 (**D**, **I**) and 30 (**E**, **J**) at LL (upper panel, A–E) and at HL (lower panel, F–J) conditions. Each curve represents a thermal performance curve (TPC) fit to the double-exponential model (Thomas *et al.*, 2017, equation (2)). The points represent μmax of independent replicates at each experimental condition ($n = 4$ for each condition). The solid line represents the mean predictions, and the shaded bands represent the 95% confidence interval of model fits.

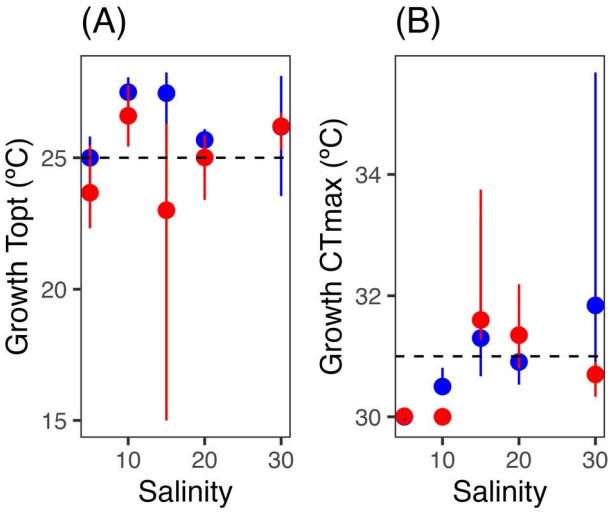

Fig. 2. Optimum temperature (Growth *Topt*, °C—Fig. 1A) and the upper thermal niche limit (growth *CTmax*, °C—Fig. 1B) for the growth of *K. veneficum* at the salinity range of 5–30 at LL (blue symbols) and HL (red symbols). The points represent the estimates from the model fits and the lines represent the 95% confidence intervals of the estimated parameters. The dashed lines in A and B are arbitrary levels of 25 and 31°C, respectively.

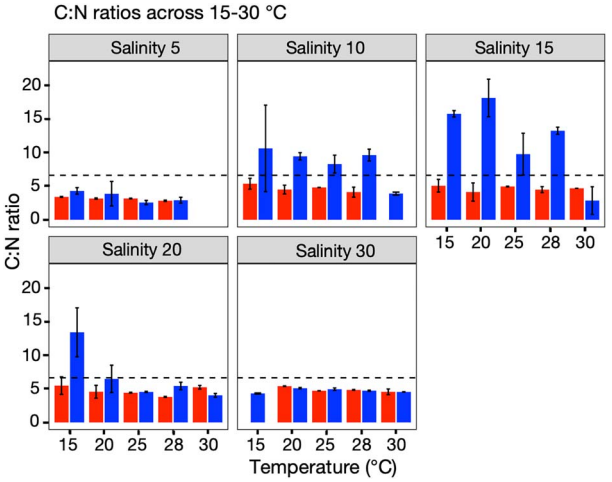

Fig. 3. Atomic ratios of C:N of *K. veneficum*, across 15–30°C at the salinities 5, 10, 15, 20 and 30 at LL (blue bars) and HL (red bars). Errors denote the standard deviations of two replicates ($n = 2$). The dashed line represents the Redfield atomic ratio for C:N.

significantly higher C:N ratios were found for 15°C and at LL (Tukey's HSD, $P < 0.01$ compared to all other treatments at salinity 20), while no variation was found across the other treatments. Overall, higher C:N ratios were found for cells grown at the mid-salinity range (salinity 10–20), and lower temperatures (15–20°C) at LL, and this trend was caused by the significant variation of N cell quota, rather than C cell quota (Table SIII). Furthermore, all C:N ratios found for HL were well below the Redfield ratio (Fig. 3).

Relationship of *in situ* bloom occurrence with temperature and salinity

A total of 140 *K. veneficum* records were found for the period of 2016–2017 across the Chesapeake Bay. Of the total records, 18 were Type I, 51 were Type II and 71 were Type III blooms. The high biomass Type I blooms occurred at the temperatures <10–29°C and the percent bloom occurrence increased with increasing temperature, peaked at 25–29°C (33% of blooms), and no bloom records were found at >30°C (Fig. 4A). Type II blooms showed the same relationship with temperature with peak bloom occurrence at 25–29°C (32%), and a

Downloaded from https://academic.oup.com/plankt/article/45/4/604/7192951 by National Oceanic & Atmospheric Administration user on 18 March 2025

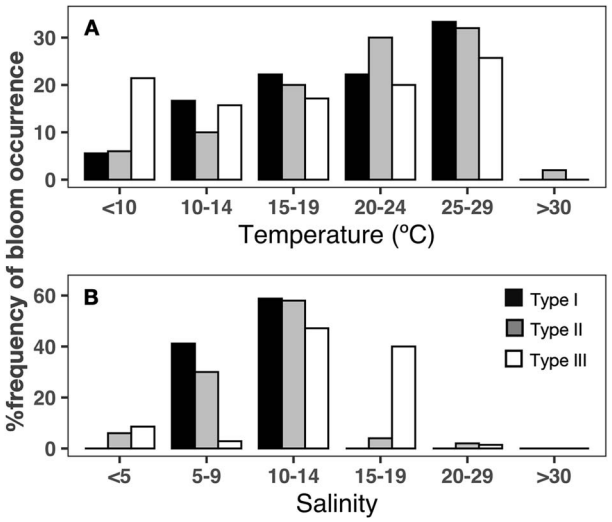

Fig. 4. Percent frequency of *K. veneficum* bloom occurrence with water temperature (**A**) and salinity (**B**) collected during 2016–2017 in the Chesapeake Bay. Data were obtained from the Bay program (https://www.chesapeakebay.net/what/data).

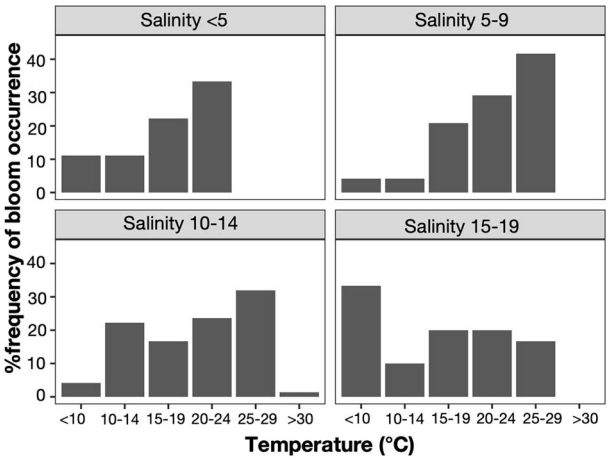

Fig. 5. Thermal preference of *K. veneficum* blooms occurred at different salinity ranges (<5, 5–9, 10–14, 15–19) in the Chesapeake Bay during 2016–2017. Not reported here are two bloom records found for salinity 20–29. Data were obtained from the Bay program (https://www.chesapeakebay.net/what/data).

sharp decrease to 2% at >30°C. In contrast, the low biomass Type III blooms occurred at <10–29°C but did not show a clear relationship with temperature (Fig. 4A). The three different bloom types also showed a distinct relationship with salinity (Fig. 4B). Type I blooms only occurred at the 5–14 salinity range, while Type II and III blooms occurred at a broader range of salinity from <5 to 29. All the bloom types peaked at the salinity range of 10–14 (59% of Type I, 58% of Type II and 47% of Type III). Furthermore, 40% of Type III blooms occurred at the salinity range of 15–19 in contrast to Type I and Type II. At salinity >30, only two bloom records were reported.

The temperature preference clearly varied with the salinity in the Chesapeake Bay data (Fig. 5). At salinity <5, bloom occurrence was more common at 20–24°C, while at salinities of 5–14, bloom occurrence was higher at 25–29°C. Furthermore, the temperature tolerance of *K. veneficum* at salinity 10–14 was higher (i.e. <10–>30°C) than at other salinity ranges. However, the percent frequency of bloom occurrence at salinity 10–14 decreased sharply from 32% at 25–29°C to 1.4% at >30°C. At the salinities above 15, the thermal preference did not show a clear trend and the highest bloom frequency was found at temperatures <10°C.

DISCUSSION

The variation of fundamental physical niche properties (temperature, salinity and light) experimentally imposed herein had a broad range of effects on growth and cell stoichiometry (C and N quota and ratios) of *K. veneficum* as well as on their thermal niche properties. Resource availability (e.g. HL in this case) can have contrasting effects on the actual trait value (e.g. growth) and on the thermal niche properties as evident from the higher growth rates but lower thermal optima for growth at the HL compared to the LL condition.

Growth-thermal response of *K. veneficum*

The growth of *K. veneficum* showed typical left-skewed unimodal thermal performance curves (TPCs) under all the conditions tested, as found previously for this species and other phytoplankton (e.g. Baker *et al.*, 2009; Thomas *et al.*, 2017; Barton and Yvon-Durocher, 2019; Vidyarathna *et al.*, 2020). Trait values and the TPC parameters greatly varied across different conditions, however.

Previous laboratory studies that reported similar temperature (Lin *et al.*, 2018b; Vidyarathna *et al.*, 2020) and salinity (Adolf *et al.*, 2009) preferences for *K. veneficum* strains originating from the mid-Atlantic regions agree with results here. The early work by Nielsen and Tønseth (1991) and Nielsen (1996) on *K. veneficum* (as *Gymnodinium galatheanum*) and a similar dinoflagellate species, *Gyrodinium aureolum*, reported that both temperature and salinity significantly affected their growth and thermal optima. While both species were able to grow at temperatures as low as 7–12°C, the thermal optima for growth were 21–24°C, which was slightly lower than the levels found herein, largely due to the differences in the species/strains and their history of thermal acclimation at different waters. The salinity optima for growth (23–29 salinity) reported in Nielsen and Tønseth (1991) and

Downloaded from https://academic.oup.com/plankt/article/45/4/604/7192951 by National Oceanic & Atmospheric Administration user on 18 March 2025

Nielsen (1996), on the other hand, were higher than the levels reported herein. These studies, however, did not investigate the growth at temperatures above their *Topt*, and therefore, the upper thermal niche boundaries for the growth of these species were not reported.

Trends in growth are likely a result of interactive effects of light with temperature and salinity rather than isolated effects. Here, HL either had no or minimal effects at temperatures below 20°C and negative effects at temperatures above 28°C at all salinity levels except 15 and did not offset the negative effects of temperature and salinity extremes on growth. Similar light temperature interactions have been reported for *Chaetoceros wighamii*, wherein a temperature increase from 7 to 11°C increased the cell growth more at a moderate light than at HL (Spilling *et al.*, 2015). A recent study, on the other hand, reported that the light availability increased the growth of *K. veneficum* at 30°C at a greater magnitude than those at 25°C (Coyne *et al.*, 2021), which was likely due to the long adaptation period of that study rather than a plasticity response found in our study. Evolved lineages of phytoplankton often exhibit higher growth responses to temperature increase as a result of adaptation compared to short-term acclimated cultures (Baker *et al.*, 2018; Strock and Menden-Deuer, 2021; Lepori-Bui *et al.*, 2022).

The TPC parameters derived from the double-exponential model estimates, however, revealed distinct trends both between the parameters (i.e. thermal optima (*Topt*) and upper thermal boundary (*CTmax*)) and across environmental gradients. First, within the preferred salinity range, the cultures grown at LL, but not those at HL, seemed to benefit from a temperature increase. As such, the hypothesis that *K. veneficum* at HL will likely be more resistant to temperature increase was not supported. A simultaneous increase of photosynthetic rates and autotrophic growth rates in response to temperature increase from 25 to 30°C at LL, but not at HL, have been reported for other phytoplankton species (e.g. *Ochromonas* sp.) as well (Lepori-Bui *et al.*, 2022). Second, the highest *CTmax* was found for salinity 30, well above their preferred range for growth. Furthermore, at LL *CTmax* showed a linear increasing trend from low to high salinity, which indicated that the cells grown at higher salinity probably were more resilient to temperature increase. Third, unlike the patterns found for *Topt*, values of *CTmax* within the preferred salinity range were higher at HL than at LL. This may indicate that although light-saturated growth did not increase the resilience to higher temperature in terms of bloom formation, it may help cells to survive better at higher temperature.

The fact that most high biomass blooms (i.e. Types I and II) occurred at a narrow temperature window of 25–29°C and a salinity window of 10–14 in the Chesapeake Bay were consistent with the laboratory findings herein. Furthermore, the preferred salinity range for *K. veneficum* bloom formation *in situ* seemed to be extended further toward the lower salinity range (i.e. 5–9) as opposed to the upper range (15–20) that would have been predicted based on our laboratory data. Interestingly, a higher percentage of low biomass Type III blooms and a small percentage of Type II occurred at salinity 15–29, which indicates that they can survive, but not form blooms, in the higher salinity, in keeping with the results herein with respect to the higher *CTmax* at salinity 30.

Temperature and light effects on C:N ratios and cell quotas

The C and N cell quotas and ratios of *K. veneficum* were largely a function of temperature and light rather than salinity. The experiments herein were conducted with nutrient replete media and the data were collected during the exponential phase; hence, it can be assumed that the C and N variations are solely due to the effects of experimental conditions and not due to any nutrient limitation. Within the preferred salinity range for growth, the C:N ratio showed a general decreasing trend with temperature at LL as a result of higher N cell quota. Increasing temperature often reduces phytoplankton cell sizes (Morán *et al.*, 2010; Yvon-Durocher *et al.*, 2011; Strock and Menden-Deuer, 2021), and it is not known if this N cell quota increase was an indirect effect of reduced cell sizes. However, a similar increase in C cell quota was not observed, indicating that N assimilation was upregulated when temperature increased at LL. On the other hand, different trends of cellular C, N and C:N ratios with temperature have been reported in previous studies on *K. veneficum*, including decreasing C:N ratios (Spilling *et al.*, 2015; Vidyarathna *et al.*, 2020) as well as increases in both C and N cell quotas and invariant C:N ratios with increasing temperatures (Coyne *et al.*, 2021). These discrepancies may be caused by the differences in acclimation time, nutrient sources and concentration between different studies. Within the same salinity range (10–20), the C:N ratios for cells grown at HL were significantly lower than those grown at LL likely due to the higher resource allocation to cell division at the expense of biomass under HL condition.

Implications for HAB formation in the Chesapeake Bay in a warming scenario

Estuarine systems such as the Chesapeake Bay experience daily temperature perturbations. Yet *K. veneficum* was able to adjust its physiology across a wide range of temperature and salinity, possibly through the phenotypic plasticity.

Downloaded from https://academic.oup.com/plankt/article/45/4/604/7192951 by National Oceanic & Atmospheric Administration user on 18 March 2025

Based on these results of *K. veneficum* growth and the TPC model estimates for thermal optima, it is suggested that bloom formation will likely be reduced during the warmest period of the summer due to their thermal sensitivity, specially under HL conditions. This is in agreement with the model results of Li *et al.* (2020b). However, *K. veneficum* can inhabit the water column from the surface to several meters deep and may find habitats where light is optimum, and therefore where temperature shifts are less stressful. In that case, bloom formation may prevail through the summer season as well.

These findings on higher *CTmax* at salinity beyond the preferred range are ecologically important, especially under future scenarios of sea level rise in the Chesapeake Bay. Most studies conducted on *K. veneficum* in the Chesapeake Bay so far have given only a little attention on the high salinity effect due to the fact that they usually form blooms in the upper and mid bay regions. However, at higher salinities, when the light is limited, *K. veneficum* was more resistant to temperature increase. The high salinity, lower bay regions, therefore, possibly provide "over-summering" habitats for *K. veneficum* seed populations.

Neither the habitat model of Li *et al.* (2020b), nor the current experiments account for mixotrophic feeding by *K. veneficum*. In the natural environment where prey is abundant, mixotrophy can play a significant role in its bloom formation (Li *et al.*, 2000b, 2015; Place *et al.*, 2012). A separate mechanistic model of *K. veneficum* in the Chesapeake Bay incorporating mixotrophy has been developed by Li *et al.* (2022). Not only are ingestion and digestion a function of temperature, but the growth of the prey cryptophytes is also a function of temperature and salinity. Li *et al.* (2001) estimated the rate at which *K. veneficum* digested cryptophyte prey by conducting *in silico* temperature-controlled experiments over a range of 10–29.7°C while holding other environmental conditions constant. They found that the digestion rate was strongly dependent on temperature. Model output showed that mixotrophic feeding increased in response to prey availability and to phosphorus deficiency which began late in the spring/early summer. During the warmer months of the years, growth dependence on phagotrophy was enhanced as the digestion rate increased. The factors studied here alone and in combination can have significant effects on mixotrophy and further modify their responses in a future climate change scenario and are worth investigating in future experimental and *in silico* studies. Such additional information will allow us to better link the metabolic plasticity of individual HAB species to ecosystem level and produce more robust predictions on prevalence of HABs in a future climate change scenario.

CONCLUSIONS

Under the current climate condition, combined effects of 10–20 salinity, 25–28°C and HL represent the preferred niche for bloom formation in the Chesapeake Bay, while in a warming scenario the same salinity and temperature niche with LL may be more favorable for bloom formation. Temperature increases above 28°C may suppress *K. veneficum* bloom formation in the Chesapeake Bay. The high-salinity lower bay regions may provide over-summering habitats for *K. veneficum* during warm summer months. In a warming scenario, cells with mixotrophic feeding may also be able to overcome the negative direct effects of warm waters.

ACKNOWLEDGEMENTS

We thank two anonymous reviewers for their valuable comments. We acknowledge Dr M. Warner (University of Delaware) for assistance with CHN analyses. This is contribution number 6272 of the University of Maryland Center for Environmental Science and number ECO1041 from the NOAA ECOHAB program.

SUPPLEMENTARY DATA

Supplementary data is available at *Journal of Plankton Research* online.

FUNDING

This study was supported by the National Oceanic and Atmospheric Administration (NOAA) through grant NA17NOS4780180.

DATA AVAILABILITY

The data underlying this article are available in the article and in its online supplementary material.

REFERENCES

Adolf, J. E., Bachvaroff, T. R., Deeds, J. R. and Place, A. R. (2015) Ichthyotoxic *Karlodinium veneficum* (Ballantine) J Larsen in the upper swan river estuary (Western Australia): ecological conditions leading to a fish kill. *Harmful Algae*, **48**, 83–93.

Adolf, J. E., Bachvaroff, T. R. and Place, A. R. (2009) Environmental modulation of karlotoxin levels in strains of the cosmopolitan dinoflagellate, *Karlodinium veneficum* (dinophyceae)1. *J. Phycol.*, **45**, 176–192.

Adolf, J. E., Krupatkina, D., Bachvaroff, T. and Place, A. R. (2007) Karlotoxin mediates grazing by *Oxyrrhis marina* on strains of *Karlodinium veneficum*. *Harmful Algae*, **6**, 400–412.

Baker, J. W., Grover, J. P., Ramachandrannair, R., Black, C., Valenti, T. W. Jr., Brooks, B. W. and Roelkec, D. L. (2009) Growth at the edge of the niche: an experimental study of the harmful alga *Prymnesium parvum*. *Limnol. Oceanogr.*, **54**, 1679–1687.

Downloaded from https://academic.oup.com/plankt/article/45/4/604/7192951 by National Oceanic & Atmospheric Administration user on 18 March 2025

Baker, K. G., Radford, D. T., Evenhuis, C., Kuzhiumparam, U., Ralph, P. J. and Doblin, M. A. (2018) Thermal niche evolution of functional traits in a tropical marine phototroph. *J. Phycol.*, **54**, 799–810.

Barton, S. and Yvon-Durocher, G. (2019) Quantifying the temperature dependence of growth rate in marine phytoplankton within and across species. *Limnol. Oceanogr.*, **64**, 2081–2091.

Bjørnland, T. and Tangen, K. (1979) Pigmentation and morphology of a marine *Gyrodinium* (dinophyceae) with a major carotenoid different from peridinin and fucoxanthin. *J. Phycol.*, **15**, 457–463.

Braarud, T. (1957) A red water organism from Walvis Bay (*Gymnodinium galatheanum* n. sp.). *Galathea Deep Sea. Exped.*, **1**, 137–138.

Brownlee, E. F., Sellner, S. G., Sellner, K. G., Nonogaki, H., Adolf, J. E., Bachvaroff, T. R. and Place, A. R. (2008) Responses of *Crassostrea virginica* (Gmelin) and *C. ariakensis* (Fujita) to bloom-forming phytoplankton including ichthyotoxic *Karlodinium veneficum* (Ballantine). *J. Shellfish Res.*, **27**, 581–591.

Coyne, K. J., Salvitti, L. R., Mangum, A. M., Ozbay, G., Main, C. R., Kouhanestani, Z. M. and Warner, M. E. (2021) Interactive effects of light, CO_2 and temperature on growth and resource partitioning by the mixotrophic dinoflagellate, *Karlodinium veneficum*. *PLoS One*, **16**, e0259161.

Dai, X., Lu, D., Guan, W., Wang, H., He, P., Xia, P. and Yang, H. (2014) Newly recorded *Karlodinium veneficum* dinoflagellate blooms in stratified water of the East China Sea. *Deep Sea Res. Part II Top. Stud. Oceanogr.*, **101**, 237–243.

Deeds, J. R., Terlizzi, D. E., Adolf, J. E., Stoecker, D. K. and Place, A. R. (2002) Toxic activity from cultures of *Karlodinium micrum* (=*Gyrodinium galatheanum*) (Dinophyceae)—a dinoflagellate associated with fish mortalities in an estuarine aquaculture facility. *Harmful Algae*, **1**, 169–189.

Edwards, K. F., Thomas, M. K., Klausmeier, C. A. and Litchman, E. (2016) Phytoplankton growth and the interaction of light and temperature: a synthesis at the species and community level. *Limnol. Oceanogr.*, **61**, 1232–1244.

Fox, J. and Weisberg, S. (2011) *An {R} Companion to Applied Regression*, 2nd edn, Sage, Thousand Oaks CA.

Fu, F. X., Place, A. R., Garcia, N. S. and Hutchins, D. A. (2010) CO_2 and phosphate availability control the toxicity of the harmful bloom dinoflagellate *Karlodinium veneficum*. *Aquat. Microb. Ecol.*, **59**, 55–65.

Glibert, P. M., Alexander, J., Meritt, D. W., North, E. W. and Stoecker, D. K. (2007) Harmful algae pose additional challenges for oyster restoration: impacts of the harmful algae *Karlodinium veneficum* and *Prorocentrum minimum* on early life stages of the oysters *Crassostrea virginica* and *Crassostrea ariakensis*. *J. Shellfish Res.*, **26**, 919–925.

Glibert, P. M., Cai, W.-J., Hall, E. R., Li, M., Main, K. L., Rose, K. A., Testa, J. M. and Vidyarathna, N. K. (2022) Stressing over the complexities of multiple stressors in marine and estuarine systems. *Ocean-Land-Atmosphere Res.*, **2022**, 9787258.

Guillard, R. R. L. and Ryther, J. H. (1962) Studies of marine planktonic diatoms: I. *Cyclotella nana* Hustedt, and *Detonula confervacea* (Cleve) gran. *Can. J. Microbiol.*, **8**, 229–239.

Hong, B. and Shen, J. (2012) Responses of estuarine salinity and transport processes to potential future sea-level rise in the Chesapeake Bay. *Estuar. Coast. Shelf Sci.*, **104–105**, 33–45.

Howarth, R. W. (2008) Coastal nitrogen pollution: a review of sources and trends globally and regionally. *Harmful Algae*, **8**, 14–20.

Kaushal, S. S., Likens, G. E., Utz, R. M., Pace, M. L., Grese, M. and Yepsen, M. (2013) Increased river alkalinization in the eastern U.S. *Environ. Sci. Technol.*, **47**, 10302–10311.

Lepori-Bui, M., Paight, C., Eberhard, E., Mertz, C. M., and Moeller, H. V. (2022). Evidence for evolutionary adaptation of mixotrophic nanoflagellates to warmer temperatures. *Glob. Chang. Biol.*, **2022**;**00**:1–14.

Li, A., Stoecker, D. K. and Coats, D. W. (2000a) Spatial and temporal aspects of *Gyrodinium galatheanum* in Chesapeake Bay: distribution and mixotrophy. *J. Plankton Res.*, **22**, 2105–2124.

Li, A., Stoecker, D. K. and Coats, D. W. (2000b) Mixotrophy in *Gyrodinium galatheanum* (Dinophyceae): grazing responses to light intensity and inorganic nutrients. *J. Phycol.*, **36**, 33–45.

Li, A., Stoecker, D. K. and Coats, D. W. (2001) Use of the 'food vacuole content' method to estimate grazing by the mixotrophic dinoflagellate *Gyrodinium galatheanum* on cryptophytes. *J. Plankton Res.*, **23**, 303–318.

Li, J., Glibert, P. M. and Gao, Y. (2015) Temporal and spatial changes in Chesapeake Bay water quality and relationships to *Prorocentrum minimum*, *Karlodinium veneficum*, and CyanoHAB events, 1991–2008. *Harmful Algae*, **42**, 1–14.

Li, M., Chen, Y., Zhang, F., Song, Y., Glibert, P. M. and Stoecker, D. K. (2022) A three-dimensional mixotrophic model of *Karlodinium veneficum* blooms for a eutrophic estuary. *Harmful Algae*, **113**, 102203.

Li, M., Li, R., Cai, W.-J., Testa, J. M. and Shen, C. (2020a) Effects of wind-driven lateral upwelling on estuarine carbonate chemistry. *Front. Mar. Sci.*, **7**, 588465.

Li, M., Ni, W., Zhang, F., Glibert, P. M. and Michelle Lin, C.-H. (2020b) Climate-induced interannual variability and projected change of two harmful algal bloom taxa in Chesapeake Bay, USA. *Sci. Total Environ.*, **744**, 140947.

Lin, C.-H., Flynn, K. J., Mitra, A. and Glibert, P. M. (2018b) Simulating effects of variable stoichiometry and temperature on mixotrophy in the harmful dinoflagellate *Karlodinium veneficum*. *Front. Mar. Sci.*, **5**, 320.

Lin, C. H., Lyubchich, V. and Glibert, P. M. (2018a) Time series models of decadal trends in the harmful algal species *Karlodinium veneficum* in Chesapeake Bay. *Harmful Algae*, **73**, 110–118.

Marshall, H. G., Burchardt, L. and Lacouture, R. (2005) A review of phytoplankton composition within Chesapeake Bay and its tidal estuaries. *J. Plankton Res.*, **27**, 1083–1102.

Morán, X. A. G., López-Urrutia, Á., Calvo-Díaz, A. and Li, W. K. W. (2010) Increasing importance of small phytoplankton in a warmer ocean. *Glob. Chang. Biol.*, **16**, 1137–1144.

Muhling, B. A., Gaitán, C. F., Stock, C. A., Saba, V. S., Tommasi, D. and Dixon, K. W. (2018) Potential salinity and temperature futures for the Chesapeake Bay using a statistical downscaling spatial disaggregation framework. *Estuar. Coasts*, **41**, 349–372.

Najjar, R. G., Pyke, C. R., Adams, M. B., Breitburg, D., Hershner, C., Kemp, M., Howarth, R., Mulholland, M. R. *et al.* (2010) Potential climate-change impacts on the Chesapeake Bay. *Estuar. Coast. Shelf Sci.*, **86**, 1–20.

Ni, W., Li, M. and Testa, J. M. (2020) Discerning effects of warming, sea level rise and nutrient management on long-term hypoxia trends in Chesapeake Bay. *Sci. Total Environ.*, **737**, 139717.

Nielsen, M. V. (1996) Growth and chemical composition of the toxic dinoflagellate *Gymnodinium galatheanum* in relation to irradiance, temperature and salinity. *Mar. Ecol. Prog. Ser.*, **136**, 205–211.

Downloaded from https://academic.oup.com/plankt/article/45/4/604/7192951 by National Oceanic & Atmospheric Administration user on 18 March 2025

Nielsen, M. V. and Tønseth, C. P. (1991) Temperature and salinity effect on growth and chemical composition of *Gyrodinium aureolum* Hulburt in culture. *J. Plankton Res.*, **13**, 389–398.

Padfield, D., O'Sullivan, H. and Pawar, S. (2021) rTPC and nls.multstart: a new pipeline to fit thermal performance curves in R. *Methods Ecol. Evol.*, **12**, 1138–1143.

Place, A. R., Bowers, H. A., Bachvaroff, T. R., Adolf, J. E., Deeds, J. R. and Sheng, J. (2012) *Karlodinium veneficum*-the little dinoflagellate with a big bite. *Harmful Algae*, **14**, 179–195.

R Core Team (2021) *R: A Language and Environment for Statistical Computing*, R Found. Stat. Comput, Austria.

Raven, J. and Geider, R. (1988) Temperature and algal growth. *New Phytol.*, **110**, 441–461.

Shen, C., Testa, J. M., Li, M. and Cai, W.-J. (2020) Understanding anthropogenic impacts on pH and aragonite saturation state in Chesapeake Bay: insights from a 30-year model study. *J. Geophys. Res. Biogeosci.*, **125**, e2019JG005620.

Spilling, K., Ylöstalo, P., Simis, S. and Seppälä, J. (2015) Interaction effects of light, temperature and nutrient limitations (N, P and Si) on growth, stoichiometry and photosynthetic parameters of the cold-water diatom *Chaetoceros wighamii*. *PLoS One*, **10**, e0126308.

Stoecker, D. K., Adolf, J. E., Place, A. R., Glibert, P. M. and Meritt, D. W. (2008) Effects of the dinoflagellates *Karlodinium veneficum* and *Prorocentrum minimum* on early life history stages of the eastern oyster (*Crassostrea virginica*). *Mar. Biol.*, **154**, 81–90.

Strock, J. P. and Menden-Deuer, S. (2021) Temperature acclimation alters phytoplankton growth and production rates. *Limnol. Oceanogr.*, **66**, 740–752.

Testa, J. M., Lyubchich, V. and Zhang, Q. (2019) Patterns and trends in secchi disk depth over three decades in the Chesapeake Bay estuarine complex. *Estuar. Coasts*, **42**, 927–943.

Thomas, M. K., Aranguren-Gassis, M., Kremer, C. T., Gould, M. R., Anderson, K., Klausmeier, C. A. and Litchman, E. (2017) Temperature–nutrient interactions exacerbate sensitivity to warming in phytoplankton. *Glob. Chang. Biol.*, **23**, 3269–3280.

Vidyarathna, N. K., Papke, E., Coyne, K. J., Cohen, J. H. and Warner, M. E. (2020) Functional trait thermal acclimation differs across three species of mid-Atlantic harmful algae. *Harmful Algae*, **94**, 101804.

Wagena, M. B., Collick, A. S., Ross, A. C., Najjar, R. G., Rau, B., Sommerlot, A. R., Fuka, D. R., Kleinman, P. J. A. *et al.* (2018) Impact of climate change and climate anomalies on hydrologic and biogeochemical processes in an agricultural catchment of the Chesapeake Bay watershed, USA. *Sci. Total Environ.*, **637–638**, 1443–1454.

Waggett, R. J., Tester, P. A. and Place, A. R. (2008) Anti-grazing properties of the toxic dinoflagellate *Karlodinium veneficum* during predator-prey interactions with the copepod *Acartia tonsa*. *Mar. Ecol. Prog. Ser.*, **366**, 31–42.

Yvon-Durocher, G., Montoya, J. M., Trimmer, M. and Woodward, G. U. Y. (2011) Warming alters the size spectrum and shifts the distribution of biomass in freshwater ecosystems. *Glob. Chang. Biol.*, **17**, 1681–1694.

Downloaded from https://academic.oup.com/plankt/article/45/4/604/7192951 by National Oceanic & Atmospheric Administration user on 18 March 2025